Analysis of Energy Dissipation and Ductility of castellated Steel Links in Eccentrically braced Frame under Lateral Cyclic Loading

Desi Sandy
Civil Engineering Department, Hasanuddin University, Indonesia
sandy.mylife@yahoo.co.id (corresponding author)

Herman Parung
Civil Engineering Department, Hasanuddin University, Indonesia
parungherman@yahoo.co.id

Rita Irmawaty
Civil Engineering Department, Hasanuddin University, Indonesia
rita_irmaway@yahoo.co.id

Received: 30 January 2025 | Revised: 4 March 2025 | Accepted: 17 March 2025

 DOI: https://doi.org/10.48084/etasr.10384

ABSTRACT

High-ductility and high-strength steel is highly suitable for earthquake-affected areas. An Eccentric Braced Frame (EBF) with replaceable links is a system that provides extraordinary ductility and resistance to earthquake-induced forces. The Eccentrically Braced Frame (EBF) design aims to combine the advantages of the lateral load-resisting systems of the Moment-Resisting Frame (MRF) and the Concentrically Braced Frame (CBF) into a single structural system to resulting in a structure with high elastic stiffness and high energy dissipation during a severe earthquake. In this case, steel castellated beams are used as beam spans. Castellated beams can increase the moment of inertia (I) and reduce the weight of the element. The use of castellated beams has advantages, such as geometric efficiency, especially at long spans. The objective of this research is to analyze the behavior of EBF in steel castellated connections using an experimental method. This study analyzes two specimens, CL450 and CL870, with link lengths of 450 mm and 870 mm, respectively. The results showed that the CL870 specimen had higher strength compared to the CL450 specimen. CL870 dissipated more energy than CL450, indicating that longer links result in greater energy dissipation. Additionally, both specimens exceeded the required ductility values, with an average ductility greater than 4, demonstrating that they have good flexibility and deformation capacity. Overall, CL870 excels in terms of strength, energy dissipation, and ductility.

Keywords-EBF; castellated beam; cyclic loading; energy dissipation; ductility

I. INTRODUCTION

EBF is a force-resisting system that has been widely researched and validated through laboratory testing and real-world earthquakes. The main objective of the EBF design is to combine the advantages of the lateral load-resisting systems of the Moment-Resisting Frame (MRF) and the Concentrically Braced Frame (CBF) into a single structural system to obtain a structure with high elastic stiffness and high energy dissipation during a severe earthquake. EBFs were first studied in [1-2]. Authors in [3-5] conducted collaborative research using numerical analysis and experiments. In 1988, EBF was officially adopted into the Uniform Building Code [6] and later incorporated in AISC 341-10 [7].

In the case of EBFs, the beam links are classified into short, intermediate, and long links based on the ratio of length to moment and shear capacity. Experimental and numerical tests conducted by previous researchers have shown that short links provide high ductility and stability in resisting earthquake loads. However, architectural requirements for openings sometimes make the selection of short links insufficient. Consequently, research into the length of links was developed, including links that experience flexural yielding [4].

Bracing is a structural component in a steel structure used to resist earthquake forces. It thus prevents excessive deformation in the building structure of the steel frame system. Bracing is used to increase stiffness and reduce the impact of lateral forces due to earthquakes [8]. Brace elements behave as trusses, which withstand only tensile or compressive forces.

They are capable of minimizing the magnitude of horizontal displacement and increasing the base shear capacity of the structure. This reduces the likelihood of crack formation at beam-column connections, thereby preventing structural failure. The use of braces is intended to resist lateral forces that affect the structure during an earthquake, which are not only resisted by the beam and column elements of the structure but also resisted by the brace system [9].

Steel with high-ductility and high-strength is suitable for earthquake-prone areas, although it is relatively more expensive than other construction materials. Therefore, an optimization strategy involves using castellated beams, which increase the moment of inertia (I) without increasing weight; however at the risk of buckling under high shear forces. Castellated beams are steel beams with circular or hexagonal openings in the body (web) along the beam span at certain intervals [10]. To prevent buckling, adding diagonal reinforcement in the web openings can increase the shear capacity [11-12]. Castellated beams enhance structural performance by creating stronger cross-sections that resist higher loads [13]. The objective of this study is to analyze the behavior of eccentrically braced frame structures using castellated steel beams under lateral cyclic loading.

II. MATERIAL AND METHODS

A. Design of Specimen

The material used in this study is steel with an ultimate strength of 370 MPa (BJ 37), a beam span of 4000 mm, and a frame height of 3000 mm. To model the EBF, the beams selected have two variations in link length: CL450 with a link length of 450 mm and CL870 with a link length of 870 mm. The EBF portal structural elements use steel profiles, with columns using H-shaped 200×200×8×12 mm profiles (H×B×tw×tf), link beams and non-link beams using IWF 150×75×7×5 profiles, and bracing using UNP 100×50×5 profiles. All dimensions are in mm. The test specimen configurations are illustrated in Figures 1 and 2.

After construction, the castellated beam link test specimens were examined against the test specimens, including measurements of the castellated link beam height (d_g), profile cutting height (H), wing width (b_f), web thickness (t_w),and flange thickness (t_f). The cross-sectional profile data showed that the IWF150 profile was modified into a castellated steel profile without any reduction in weight but with an increase in height. Therefore, the moment of inertia (*I*) increased. Based on the height and moment of inertia (I) value, it was found that the IWF200 profile had a moment of inertia nearly equal to that of the castellated profile. Additionally, the IWF 200 profile was heavier than the castellated steel profile. The castellated steel profile data are provided in Table I, while the IWF 200 profile data are displayed in Table II.

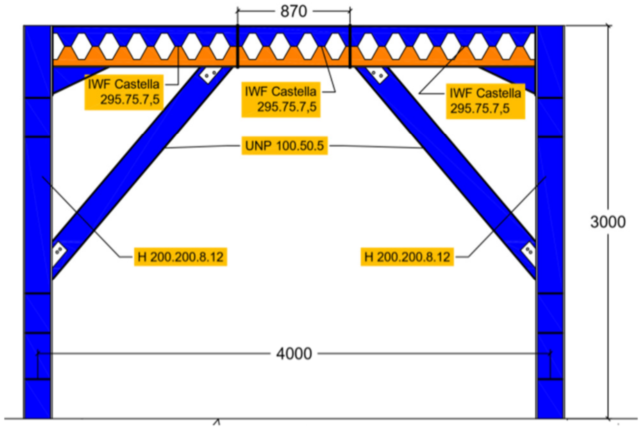

Fig. 1. Modeling of the CL450 specimen.

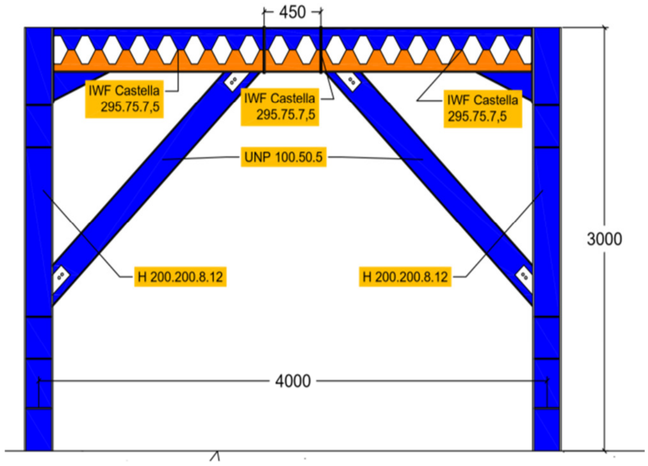

Fig. 2. Modeling of the CL870 specimen.

TABLE I. DIMENSIONS OF THE STANDARD IWF 150×75×5×7 STEEL PROFILE

Dimensions of normal steel profile		
b_f	mm	75
H	mm	150
t_f	mm	7.0
t_w	mm	5.0
A	mm^2	1785
I_x	mm^4	$6.66{\times}10^6$
S_x	mm^3	$18.4{\times}10^4$
W	kg/m	14

TABLE II. DIMENSIONS OF CASTELLATED STEEL

Dimensions of castellated steel		
b_f	mm	75
h_o	mm	295
t_f	mm	7.0
t_w	mm	5.0
A	mm^2	2525
I_x	mm^4	$29.21{\times}10^6$
Ø	Degrees^0	60
W	kg/m	14

B. Test Setup and Loading Protocol

Figure 3 illustrates the modeling setup. The portal end of the specimen was connected to an actuator operating in tension-compression motion in a direction perpendicular to the axis of the link beam. The link was connected to the beam using bolts and thick plates. Loading was applied through the actuator at the upper end of the link in the form of a quasi-static cyclic-displacement set to follow a predetermined loading pattern. Instruments, such as strain gauge and Linear Variable Displacement Transducer (LVDT), were installed. Strain gauges measured strain at their installation points. LVDTs recorded the displacements that occurred at the strain gauge installation points. The LVDT is a device used to measure displacement at its installation location The magnitude of the applied load, the displacement of the upper end of the link, and the strain on the link, namely the axial strain on the flange plate and the shear strain on the link body plate, were recorded during loading. The loading was stopped when a decrease in the peak load reading of the loading cycle was observed, which also indicated the failure of the specimen.

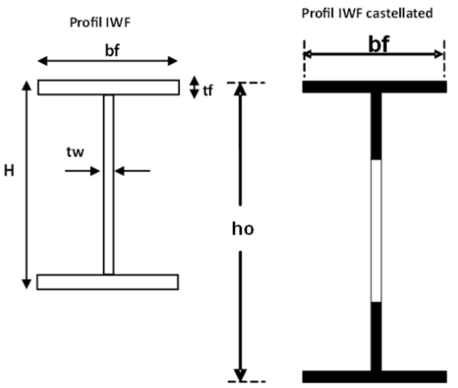

Fig. 3. IWF Profile and castellated profile.

Fig. 4. Laboratory testing setup.

The loading protocol listed in AISC 2005 [14] was used to define the load as a function of displacement on the specimen. An initial displacement of 0.16 mm was applied during the first cyclic loading cycle. Loading was then progressively increased until the link failed. The loading protocol, depicted in Figure 5, was implemented on the EBF portal link CL450 and indicated that the maximum cyclic tensile load should be 132.835 kN, and the compressive load was 126.96 kN at Cycle 13. Figure 6 shows that the peak tensile cyclic load was 159.735 kN, while the peak compressive load was 138.195 kN, both occurring at Cycle 33.

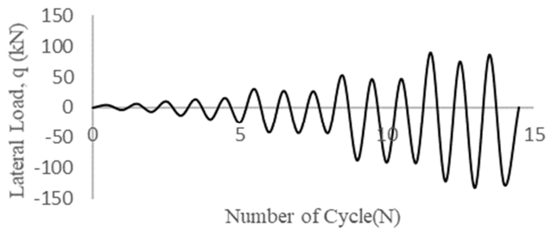

Fig. 5. Loading protocol for CL450.

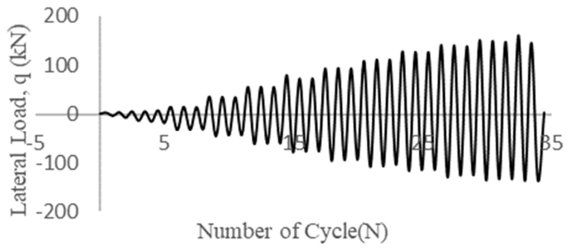

Fig. 6. Loading protocol for CL870.

III. RESULT AND DISCUSSION

A. Steel Tensile Test Results

This experiment includes testing the tensile strength of steel profiles using a single specimen with a plate thickness of 12.5 mm. The tensile strength of the IWF 150×75×8×5.5 steel profile is presented in Table III.

The IWF150 profile was modified into a castellated steel profile, increasing its height without any observed weight reduction. This modification increased the moment of inertia (I). When comparing the height and moment of inertia (I) of the castellated steel profile to the IWF200 profile, it was found that the IWF200 profile has almost the same moment of inertia (I) but a greater weight than the castellated steel profile.

TABLE III. TENSILE TEST RESULTS OF STEEL PROFILE IWF 150×75×8×5.5

Sample plate	fy	fu	P_{max}	E
	(N/mm²)	(N/mm²)	kN	MPa
t = 12.5	502.7	542.44	55.53	200000
	502.4	542.10	55.49	200000

B. Lateral Load-Displacement Relationship

The CL450 specimen has a link length of 450 mm. Based on the results of the cyclic-load test conducted in the laboratory, the hysteresis curve combines lateral load and displacement data, as shown in Figure 7. The results of the hysteresis curve exhibit that the CL450 test specimen is able to resist the lateral load of 119.786 kN when the displacement is 45.675 mm. This occurred in Cycle 14, when specimen failure prompted test termination, and the loading was stopped.

Initial yielding occurred in Specimen CL450 in the 9th Cycle, during which the displacement was 4.5 mm. The former took place when the specimen resisted a lateral load of 55.70 kN. The specimen failed during the 13th Cycle, when the specimen was subjected to a displacement of 34.157 mm with a lateral load of 135.673 kN.

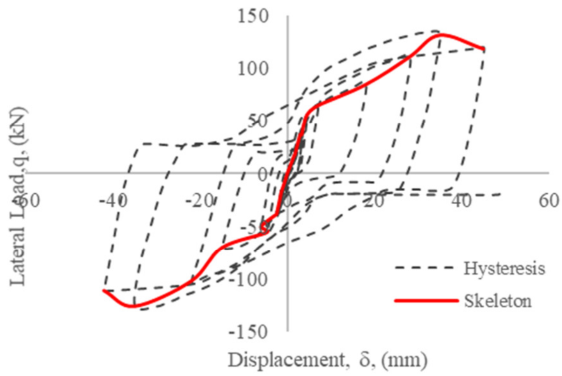

Fig. 7. Hysteresis curves of CL450.

Based on the results of the cyclic load test conducted in the laboratory for the CL 870 specimen, which has a link length of 870 mm, the hysteresis curve, as can be seen in Figure 8, combines lateral load and displacement data. The results of the hysteresis curve demonstrated that the CL870 specimen could resist the lateral load of 150.246 kN when it experienced a displacement of 50.625 mm. This occurred in Cycle 34, when specimen failure prompted test termination, and the loading was stopped.

Specimen CL870 experienced initial yielding at the 9th Cycle, where the displacement was 4.5 mm. The initial yield occurred when the specimen resisted a lateral load of 55.7 kN. The specimen failed during the 33rd cycle, when it had displacement of 48.26 mm with a lateral load was 159.735 kN.

C. *Strength of Specimen*

Strength is the maximum lateral force (shear force) the specimen can withstand at each loading step.The experimental results are presented in Table IV. The data show that CL870 obtained the highest strength in resisting tension and compression compared to CL450.

TABLE IV. MAXIMUM LATERAL LOAD AND MAXIMUM DISPLACEMENT

Specimen	Maximum lateral load (kN)	Failure load (kN)	Maximum displacement (mm)
CL450 +	135.673	119.786	45.675
CL450 -	-126.331	-111.338	-41.274
CL870 +	159.735	150.246	50.625
CL870 -	-138.195	-130.345	-50.456

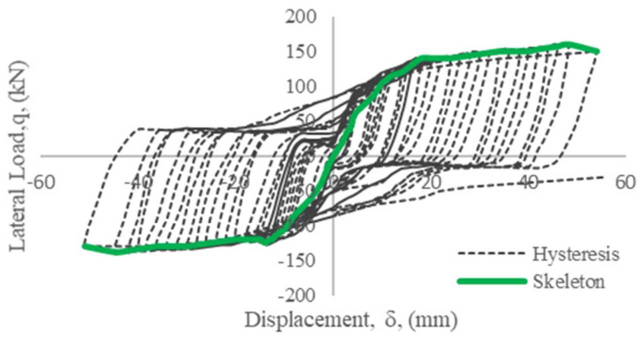

Fig. 8. Hysteresis curves of CL870.

D. *Stiffness Degradation*

The stiffness is the ratio between the maximum lateral load and displacement at each load-step. As with the strength analysis, the stiffness of both specimen models was observed during both tensile and compressive loading. The cyclic loading of the structure resulted in fatigue and reduced the strength of the structure. The portal was subjected to thrust loads, which caused rightward displacement, leading to joint cracking. During unloading, the portal was unable to return to the initial position. Cyclic right-left displacements induced fatigue, with stiffness degrading progressively over loading cycles. Where the stiffness of the portal degrades with each repeat cycle of loading./The portal stiffness degraded during each loading cycle. The stiffness degradation (DR) is presented as a stiffness ratio, which is the ratio of elastic stiffness (k_0) to secant stiffness (k_s) [15-16].

Figure 9 illustrates stiffness degradation. Specimens CL870 showed greater stiffness degradation than CL450, indicating that CL450 maintained a higher level of stiffness during testing.

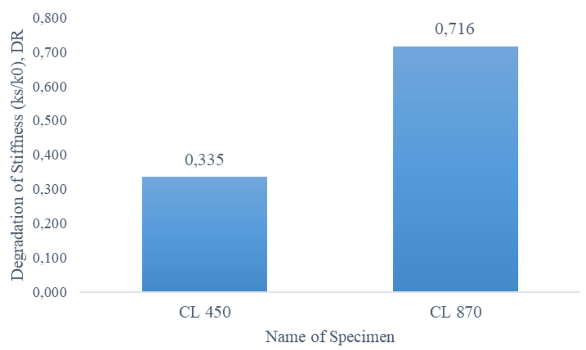

Fig. 9. Energy dissipation of CL450.

E. *Energy Dissipation*

In this study, the total energy dissipation is quantified as the area under the cyclic hysteresis curve. This is derived from the lateral load-displacement relationship. The area under the hysteresis curve is analyzed using the incremental method, where the curve is divided into several parts. Total energy dissipation is the result of the total cumulative value of the hysteretic curves generated at each loading stage. Figure 10 illustrates the energy dissipation capacity for CL450 (4306.250 kN-mm at Cycle 13), while Figure 11 for CL870 (7577.649 kN-mm at Cycle 33).

The comparison between the cumulative dissipation energy that occurs in specimens CL450 and CL870 is displayed in Figure 12. Authors in [3] stated that the EBF model includes a link beam element, where plastic hinges and collapse mechanisms are expected to localize. The shorter the link is, the greater is the effect of shear force (shear yielding) on inelastic behavior. According to [17], during an earthquake, structural elements that have high ductility will absorb significantly more energy than structural elements with small ductility. Structural ductility can be achieved by limiting the effect of earthquake energy on the structure, so that it can be absorbed and dissipated through inelastic-mechanisms.

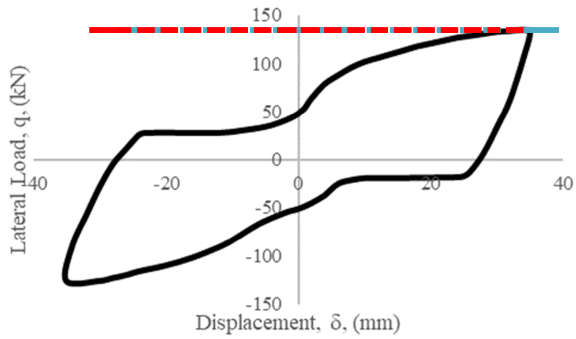

Fig. 10. Energy dissipation of CL450.

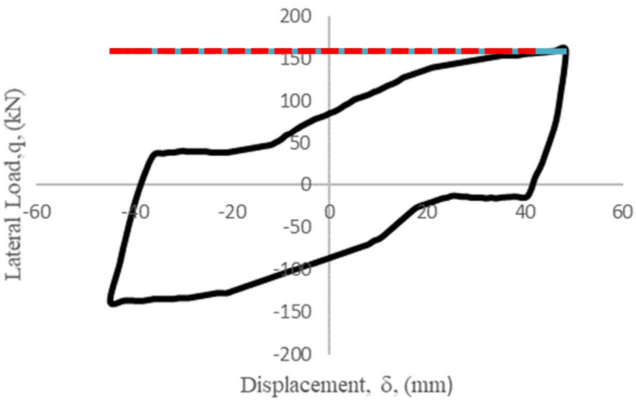

Fig. 11. Energy dissipation of CL450.

F. *Ductility of Specimen*

Authors in [18] define ductility as the ability of a structure to undergo large-amplitude cyclic deformations in the inelastic range without a substantial reduction in strength. Mathematically, ductility (μ) is expressed as the ratio of the maximum allowable deformation of the structure (μu) to the deformation at initial yielding of the structure under examination (μy) [18]. Figures 13 and 14 present the initial yield and ultimate conditions of each specimen to calculate the ductility value.

Tables V and VI summarize each specimen's initial and ultimate yield value and ductility value. Figure 15 provides the comparison between the ductility value and the link length.

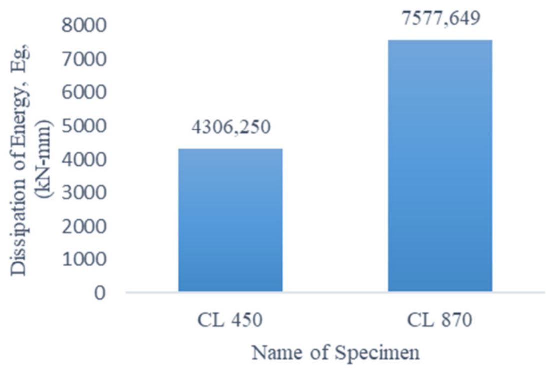

Fig. 12. Comparison of dissipation of energy.

TABLE V. INITIAL YIELD AND ULTIMATE YIELD OF CL450

	Number of cycles	Displacement (mm)	Lateral loading (kN)	Ductility
Initial Yield	9	4.5	55.7	7.78
Ultimate yield	13	34.157	135.673	

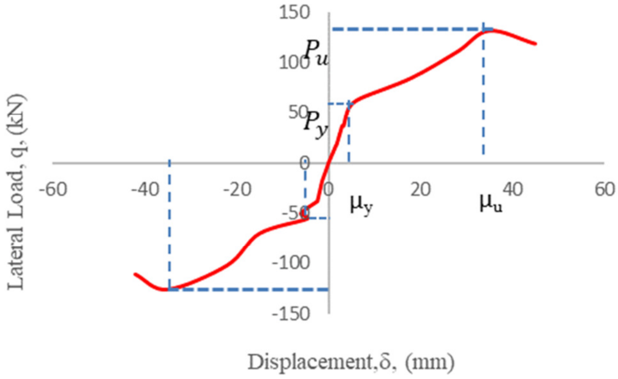

Fig. 13. Skeleton of CL450.

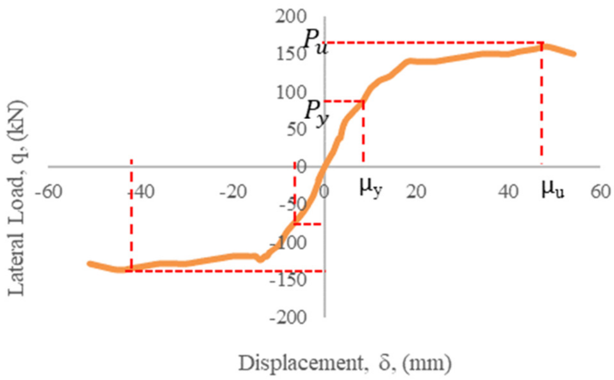

Fig. 14. Skeleton of CL870.

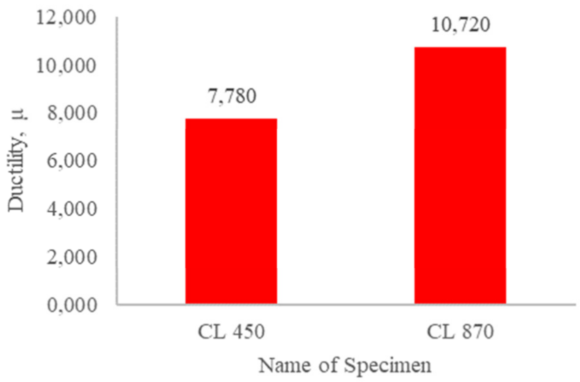

Fig. 15. Comparison of ductility.

TABLE VI. INITIAL YIELD AND ULTIMATE YIELD OF CL870

	Number of cycles	Displacement (mm)	Lateral loading (kN)	Ductility
Initial yield	9	4.5	55.7	10.72
Ultimate yield	33	48.26	159.735	

IV. CONCLUSION

Based on the experimental results, it was observed that CL870 specimens had higher strength in resisting tension and compression compared to CL450 specimens. However, CL870 exhibited greater stiffness degradation, whereas CL450 retained higher stiffness during testing. CL870 demonstrated superior energy dissipation, dissipated more energy than CL450, indicating that longer links result in greater energy dissipation. In addition, both specimens exceeded the required ductility value, with an average ductility higher than 4, suggesting that they have high ductility and deformation capacity under loading. Overall, CL870 excels in terms of strength, energy dissipation, and ductility.

ACKNOWLEDGMENT

The Authors would like to thank Structure Laboratory team of Hasanuddin University.

REFERENCES

[1] M. Fujimoto, T. Aoyagi, K. Ukai, A. Wada, K. Saito, "Structural Characteristics of Eccentric K-Braced Frames," *Transactions of the Architectural Institute of Japan*, vol. 195, pp. 30-49, 1972.

[2] R. Tanabashi, K. Naneta, T. Ishida, "On the Rigidity and Ductility of Steel Bracing as Semblage," *Proceedings of the 5th World Conference on Earthquake Engineering*, Rome, Italy, 1974.

[3] E. P. Popov, K. Kasai, M. D. Engelhardt, "Advances in Design of Eccentrically Braced Frames," *Bulletin of the New Zealand Society for Earthquake Engineering*, vol. 20, no. 1, pp. 9-22, 1987, http://doi.org/10.5459/bnzsee.20.1.22-29.

[4] J. M. Ricles, E. P. Popov, "Inelastic Link Element for EBF Seismic analysis," *Journal Structure Engineering*, *ASCE*, vol. 120, no. 2, pp. 63-441, 1994, https://doi.org/10.1061/(ASCE)0733-9445(1994)120:2(441).

[5] K. Kasai, E. P. Popov, "*General Behaviour of WF Steel Shear Link Beams*," *Journal Structure Engineering*. vol. 112, no. 2, pp. 82-362, 1985, https://doi.org/10.1061/(ASCE)0733-9445(1986)112:2(362).

[6] *Uniform Building Code (UBC)*, International Conference of Building Officials, 1988.

[7] *Seismic Provisions for Structural Steel Buildings, Vol. 341-10*, Chicago, Il, USA: American Institute for Steel Construction (AISC), 2010.

[8] A. Panuluh, "Analisa Penggunaan Sistem Rangka Bracing Terhadap Perpindahan Lateral Portal Baja Bertingkat Tinggi," Universitas Muhammadiyah Malang, 2010.

[9] B. S. Smith, A. Coull, *Tall Building Structures: Analysis and Design*, New York, NY, USA: John Wiley & Sons, Inc, 1991.

[10] M. R. Soltani, A. Bouchair, and M. Mimoune, "Nonlinear FE analysis of the ultimate behavior of steel castellated beams," *Journal of Construction Steel Research*, vol. 70, pp. 101–114, 2011, https://doi.org/10.1016/j.jcsr.2011.10.016.

[11] R. Frans, H. Parung, D. Sandy, S. Tonapa, "Numerical Modelling of Hexagonal Castellated Beam under Monotonic Loading," in *Precedia Engineering*, vol. 171, pp. 781-788, 2017, https://doi.org/10.1016/j.proeng.2017.01.449.

[12] A. C. Dhage, K. B. Pimpale, A. S. Danole, "Study of Castellated Beam Stiffened by Diagonal Andring Stiffners," *International Journal Of Engineering Research & Technology*, vol. 10, no. 8, Aug, 2021, https://doi.org/10.17577/IJERTV10IS080161.

[13] A. Ahmed, A. M. I. Said, "The Effect of Opening Size and Expansion Ratio on the Flexural Behavior of Hot Rolled Wide Flange Steel Beams with Expanded Web," *Engineering, Technology & Applied Science Research,* vol. 14, no. 1, pp. 13033-13040, 2024, https://doi.org/10.48084/etasr.6698.

[14] *ANSI/AISC 360-16, Specification for Structural Steel Buildings,* Chicago, IL, USA: American Institute of Steel Construction, 2016.

[15] S. Timoshenko and J. N Goodier, *Theory of Elasticity*, Toronto, Canada: McGraw-Hill, 1934.

[16] R. Bansal, *Strength of Materials*, New Delhi, India: Laxmi Publication (P) Ltd, 1996.

[17] T. Paulay, "Seismic Design for Torsional Response of Ductile Buildings," *Bulletin OF The New Zealand National Society For Earthquake Engineering,* vol. 29, no. 3, 1996.

[18] R. Park and T. Paulay, *Reinforcement in Concrete Design*, New York, NY, USA: Wiley, 1975.